Journal of Biomedical Optics

SPIEDigitalLibrary.org/jbo

Studies of tropical fruit ripening using three different spectroscopic techniques

Hao Zhang
Jing Huang
Tianqi Li
Xiuxiang Wu
Sune Svanberg
Katarina Svanberg

SPIE

Studies of tropical fruit ripening using three different spectroscopic techniques

Hao Zhang,[a] Jing Huang,[a] Tianqi Li,[a] Xiuxiang Wu,[a] Sune Svanberg,[a,b] and Katarina Svanberg[a,b,*]
[a]South China Normal University, Center for Optical and Electromagnetic Research, University City Campus, Research Building 5, 510006 Guangzhou, China
[b]Lund University, Lund Laser Center, SE-221 00 Lund, Sweden

Abstract. We present a noninvasive method to study fruit ripening. The method is based on the combination of reflectance and fluorescence spectroscopies, as well as gas in scattering media absorption spectroscopy (GASMAS). Chlorophyll and oxygen are two of the most important constituents in the fruit ripening process. Reflectance and fluorescence spectroscopies were used to quantify the changes of chlorophyll and other chromophores. GASMAS, based on tunable diode laser absorption spectroscopy, was used to measure free molecular oxygen in the fruit tissue at 760 nm, based on the fact that the free gases have much narrower spectral imprints than those of solid materials. The fruit maturation and ripening processes can be followed by studying the changes of chlorophyll and oxygen contents with these three techniques. [DOI: 10.1117/1.JBO.19.6.067001]

Keywords: fruit ripening; reflectance spectroscopy; fluorescence spectroscopy; gas in scattering media absorption spectroscopy.

Paper 130880RR received Dec. 11, 2013; revised manuscript received Apr. 11, 2014; accepted for publication Apr. 11, 2014; published online Jun. 2, 2014.

1 Introduction

The ability to discriminate between mature and immature fruits is very important both for fruit customers as well as for the fruit dealers. If the fruits are immature or overmature, the structure and taste are compromised and the value is reduced. Maturity signifies a quality stage where the fruits are acceptable for purchase but not necessarily ripe and in an optimal status for consumption.[1,2] Clearly, it is important to find the ripening stage when the fruits are considered to be of the desired quality. Many kinds of fruits can be harvested when considered mature but not ripe—ripeness will follow after some storage time, and is then followed by decay processes. Generally speaking, skin color, firmness, and size are the most used maturity indices for fruits,[1,3] and are often used by customers when purchasing the fruits. However, such assessments lack a fully reliable identification of the fruit ripening stage. Therefore, other biochemical and physiological parameters should be considered to determine the optimal fruit harvesting/consumption time. Sugar concentration, acidity, and starch content are the customary indices used to determine fruit ripening.[1,4] However, they cannot provide all the information needed to accurately identify the fruit ripening stage. Moreover, invasive methods are generally used to analyze these parameters to evaluate the fruit ripening.

In recent years, visible-near-infrared (vis-NIR) spectroscopy has been shown to be a promising, nondestructive method to evaluate fruit ripening, since it provides reliable information on internal characteristics of various fruit species.[5–7] However, this approach requires a very complex processing of data to build up calibration and prediction models.[8] Based on the vis-NIR spectroscopy, a simple and easy to perform measurement method, the "index of absorbance difference (I_{AD})" technique that strongly correlates with the chlorophyll content and the ethylene production of fruits, was introduced for nectarine and peach fruits.[9–11] However, this method cannot provide the precise days for the fruit ripening stage. Furthermore, it cannot differentiate the ripeness stage from the maturity of the fruits. In the present article, we demonstrate a noninvasive combination optical method based on reflectance and fluorescence spectroscopies together with the gas in scattering media absorption spectroscopy (GASMAS) technique, to study the ripening period of tropical fruits. The study focuses on measuring the changes of chlorophyll content using reflectance and fluorescence spectroscopies, and the changes of oxygen content using the GASMAS technique.

Chlorophyll is an essential pigment of fruits and is involved in fruit coloration, influencing the variations of color from green to yellow or red, when additional pigments are formed. For most fruits, the color will change during the ripening process. Therefore, the chlorophyll concentration is a major indicator of the physiology in fruit maturation/ripening. Usually, chlorophyll analysis is performed with spectrometry, including reflectance and fluorescence spectroscopies.[12–14] Thus, such techniques could be attractive tools to qualitatively estimate the changes of chlorophyll content in the fruit ripening process.

Molecular oxygen is a biologically active gas, and the oxygen concentration in fruits is of crucial importance for the ripening process and the quality of the fruits. Oxygen availability influences metabolic respiration, which leads to the synthesis of organic matter and the energy generation needed for the life processes. A common way to analyze gases *in situ* is to use absorption spectroscopy, which employs a narrow-band light source interrogating a fixed-length gas cell in combination with the use of the Beer-Lambert law. However, in porous materials such as fruits, the light is heavily scattered, which results in an undefined absorption path length. To handle this problem, the nonintrusive and easily implemented technique GASMAS was

*Address all correspondence to: Katarina Svanberg, E-mail: katarina.svanberg@med.lu.se

introduced, which is based on tunable diode laser absorption spectroscopy combined with wavelength modulation spectroscopy (WMS) techniques.[15] GASMAS has already been applied to the study of gas exchange in fruits.[16,17] We have now extended the use of the GASMAS technique to study the changes of oxygen content during the fruit ripening process.

2 Materials and Methods

2.1 *Materials*

Four kinds of tropical fruits were selected for the experimental measurements: nectarine (NE), mango (MG), papaya (PA), and guava (GU). All these fruits belong to a class referred to as climacteric fruits.[18] The fruits were acquired from a local market in South China, and visually nonripe samples were chosen. Each type of fruit was represented by a group of six fruits from the same batch. Representative fruits are depicted in Fig. 1(a). Each fruit was marked with a prefix and a number (e.g., NE1, NE2 etc.). This identification mark was written on a small piece of paper, which was attached to the fruit far away from the measurement location, to avoid interaction with the skin surface to be investigated. In the fluorescence monitoring, possible photobleaching had to be considered. If photobleaching occurs, the intensity of the fluorescence will be gradually reduced.[19] In order to fully eliminate residual effects of photobleaching, reflectance and fluorescence measurements were performed on the fruit, successively employing new locations as marked in the left side of Fig. 1(b). A 15×15-mm^2 area on the "equator" was selected, which appeared completely uniform with little structure on visual inspection. Within the area, nine individual measurement spots were selected. The locations for reflectance and fluorescence measurements were shifted every day to avoid "memory" from earlier measurements. The right-hand part of Fig. 1(b) shows the GASMAS injection and detection locations. It was ascertained that the distance from the injection fiber to the center of the detection was kept constant. The six fruits were divided into two groups, among which one group (such as, NE1, NE2, and NE3) was placed in an ambient temperature of 20°C and another group (such as, NE4, NE5, and NE6) at a temperature of 30°C.

2.2 *Methods*

2.2.1 *Broadband light reflectance spectroscopy*

Schematic drawings of the experimental setups used in the study are shown in Fig. 2. The setup illustrated in Fig. 2(a) was used for measurements of the reflectance spectra. Broadband light from a tungsten lamp with 130 mW output was guided to the sample with a fiber. Reflected light was captured with a reflectance probe and then transmitted to the slit of a portable miniature spectrometer (USB4000, Ocean Optics, Dunedin, Florida). Before the measurements, the system was calibrated with regard to intensity using a calibrated lamp (IES 1000,

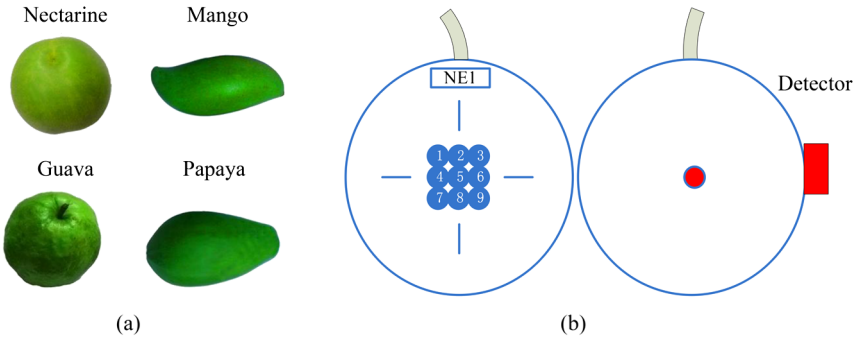

Fig. 1 The four kinds of fruits studied in the experiments (a) and a schematic drawing of the measurement locations on the fruit skin for reflectance and fluorescence measurements, and for the gas in scattering media absorption spectroscopy (GASMAS) probing. (NE1 is short for nectarine #1) (b).

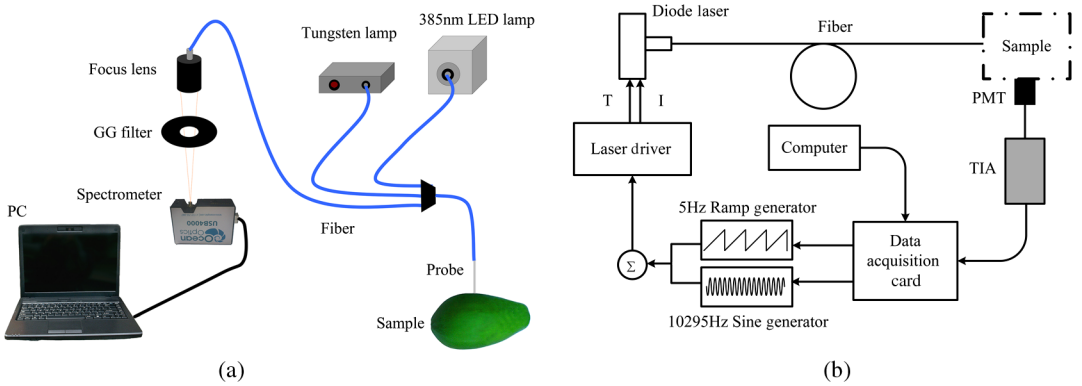

Fig. 2 Experimental arrangement for the measurements of reflectance spectra as well as the fluorescence spectra (a) and for the monitoring of the second-harmonic wavelength modulation spectroscopy (2f WMS) signal of oxygen using GASMAS (b), TIA is a transimpedance amplifier.

Labsphere, North Sutton, New Hampshire) and regarding wavelength using a low-pressure mercury lamp.

2.2.2 *Light emitting diode-induced fluorescence spectroscopy*

The fluorescence spectra were recorded with the same equipment as shown in Fig. 2(a). A 385 nm fiber-coupled UV light emitting diode was used as an excitation source and the fluorescence induced in the sample was conducted by the same fiber as employed in the reflectance measurements. The fluorescence radiation was focused on to the spectrometer entrance slit. A colored-glass filter (455 nm, Edmund, Barrington, New Jersey) was mounted in front of the spectrometer to block out the excitation light. Before the measurements, the system was again calibrated for intensity using the calibration lamp, since the presence of the colored-glass filter changed the intensity calibration.

2.2.3 *Gas in scattering media absorption spectroscopy*

The setup illustrated in Fig. 2(b) was used to attain the second-harmonic wavelength modulation spectroscopy (2f WMS) signal of oxygen. A 760 nm distributed feed-back diode laser (LD-0760-0100, Toptica, Munich, Germany) was used as the light source. Laser current and temperature controllers (LCD201C and TED 200C, Thorlabs, Newton, New Jersey) were used to control the drive current and temperature of the diode laser. The laser was spectrally scanned with a 5-Hz ramp wave over an absorption line of O_2 at 760.445 nm (vacuum wavelength), meanwhile a 10,295 Hz sinusoidal modulation was superimposed on the diode laser injection current to get a wavelength modulation of the light for sensitive modulation spectroscopy using lock-in amplification techniques. The light was then guided to the fruits through a 600 μm-core diameter optical fiber delivering an output power of 1.5 mW. A photomultiplier tube (H10722-01, Hamamatsu, Shizuoka, Japan) was used to collect the diffusely emerging light, which contains a weak absorption imprint due to oxygen. The light injection and collection locations were at positions on the fruit placed on the equator and 90 deg apart, as also indicated in Fig. 1(b). The signal received was then amplified by a current-to-voltage amplifier (DLPCA-200, Femto, Berlin, Germany) to yield a voltage signal. The voltage signal was fed to the same data acquisition card that was used to generate the modulation frequencies for the laser. The data were stored in a computer. The lock-in procedure and signal processing of the 2f WMS signal were digitally performed with a MATLAB® program, with a detailed calculating process described in Ref. 20.

3 Results and Discussion

3.1 *Reflectance and Fluorescence Measurements*

Before the spectroscopic measurements, the system was calibrated for intensity using a calibration lamp, as mentioned above. Spectral reflectance curves obtained from different stages of ripeness for each kind of fruit (NE1, MG6, GU2, and PA6) are shown in Fig. 3 (top). We observed a strong absorption at 670 to 690 nm as evidenced from the spectral shape. This is the absorption of chlorophyll which changes with the stage of ripeness. At wavelengths higher than 720 nm, the spectral shapes are almost structure-less. The chlorophyll fluorescence seen with high intensity in the red/NIR spectral region with peaks at about 685 and 740 nm was excited with UV light at 385 nm (Fig. 3, bottom). With increasing ripeness, these two fluorescence peaks change in absolute intensities, and the ratio of peak intensities was also influenced. This is related to the fact that while the 690 nm peak is reabsorbed by the chlorophyll pigment itself, this is not the case for the 740 nm peak. Thus, the latter peak grows more than the first one when the pigment concentration increases.

From the facts above, for all four kinds of fruits, the reflectance and fluorescence intensities and spectral shapes are clearly sensitive to chlorophyll content, so the reflectance and fluorescence spectra can be used as indicators to estimate the changes of chlorophyll in fruit ripening.

For getting further spectral information, more than one spectral band was studied. Thus, contrast functions were constructed to compress the multispectral information. By choosing the contrast functions to be dimensionless quantities, intensity fluctuations and other variations in the spectral measurements can be eliminated.[21] Here, we define a function R to show the changes of reflectance spectral shape with $R = (R_{720} - R_{670})/R_{720}$, where R_{670} and R_{720} are the reflectance at 670 and 720 nm, respectively. For nectarines (NE) in the two different temperature

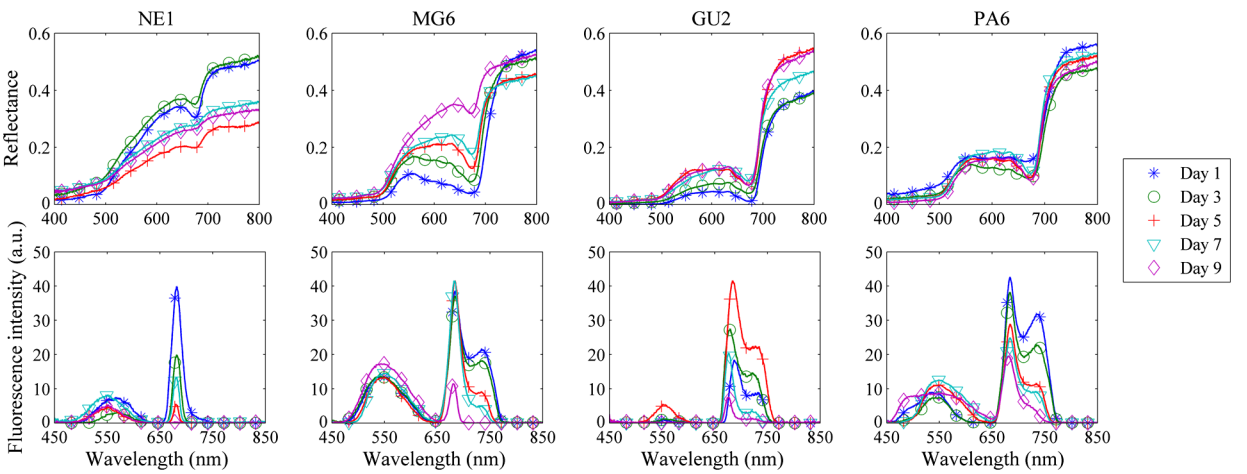

Fig. 3 Reflectance spectra (top) and fluorescence spectra (bottom) of each kind of fruit during measurement day 1, 3, 5, 7, and 9.

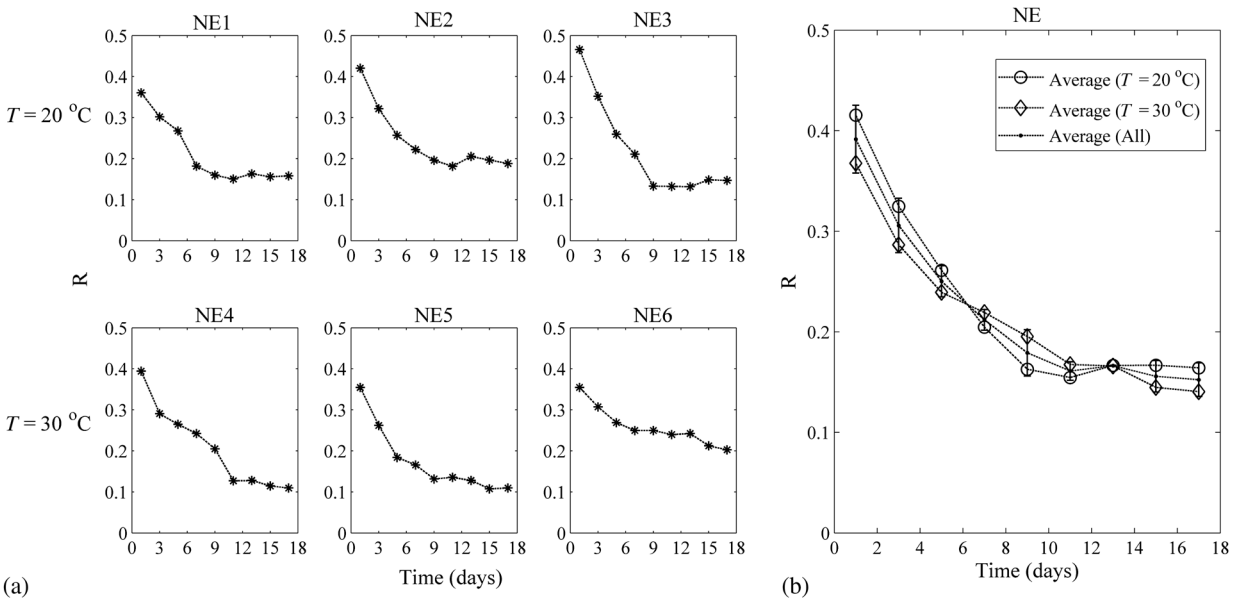

Fig. 4 The reflectance function *R* for nectarines formed from the measured data (a) and the average for different temperatures (b).

groups, the changes of R with time are shown in Fig. 4. Similarly, a function F was formed to express the changes of the fluorescence spectral shape. F is calculated as: $F = I_{740}/I_{685}$, where I_{685} and I_{740} are the fluorescence intensity values at 685 and 740 nm, respectively.[22] As discussed earlier, F is quite sensitive to the chlorophyll concentration. The time evolutions of F for NE are shown in Fig. 5.

It can be seen in Figs. 4 and 5 that the changes of R and F for NE have a similar tendency for the two temperatures (20°C and 30°C). Both functions, R and F, decrease rapidly to very low values and then stabilize. It can also be noted that the average value of R and F for the 20°C and 30°C groups have very small differences for reflectance and fluorescence, respectively [Figs. 4(b) and 5(b)]. Considering the error bars in these two figures, for most of the values of R and F, the temporal displacement of the fall-off for the two temperatures is not more than 1 day, meaning that the time for passing a chosen threshold, related to ripeness, is not more than 1 day. Although small differences are observed, we combine both temperature groups to gain higher statistical significance. The observations made for NE are also made for the three other types of fruits. The average values of R and F for the four fruit types are shown in Fig. 6. We note that while F approaches zero (the disappearance of the fluorescence peak at 740 nm), the minimum of R has a finite value since the reduction in reflectance at 670 nm due to chlorophyll [Fig. 3(a)] never becomes negligible.

The time evolution of R and F is seen to be decreasing and then arriving at a basically constant value for all the kinds of fruits, which indicates that the chlorophyll content gradually decreases to a minimum (Fig. 6). As discussed, the influence of temperature was small, but it still has some effects, which is reflected in the error bars seen in Fig. 6. Moreover, the measurement results for each fruit show some spread which is included in the error bars. The four kinds of fruits in this study are climacteric fruits. Such fruits continue to ripen after harvesting, accompanied by a color change. The skin color of

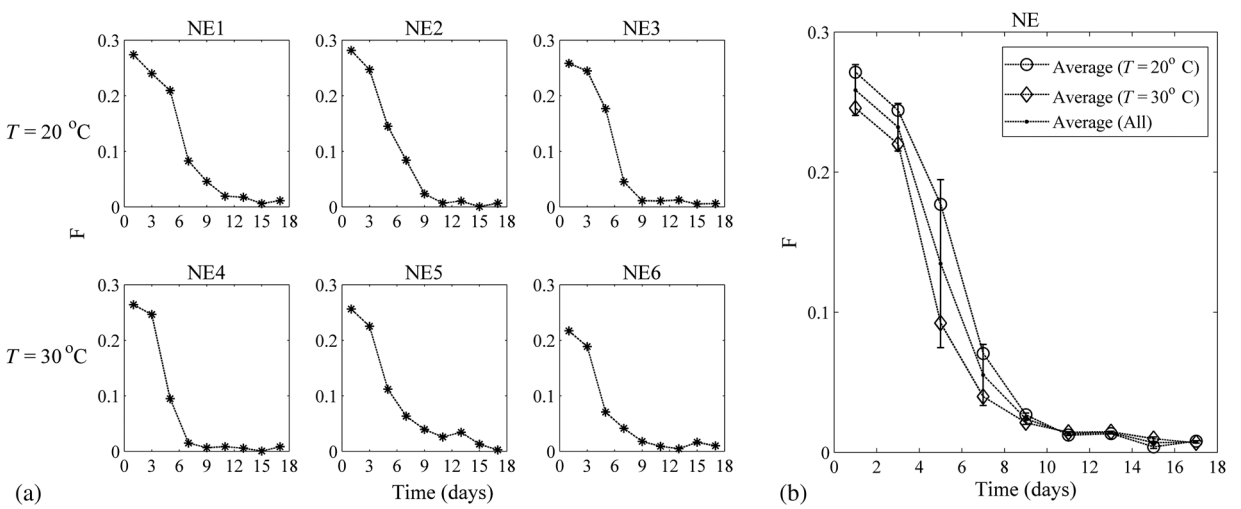

Fig. 5 The fluorescence function *F* for nectarines formed from the measured data (a) and the average for different temperatures (b).

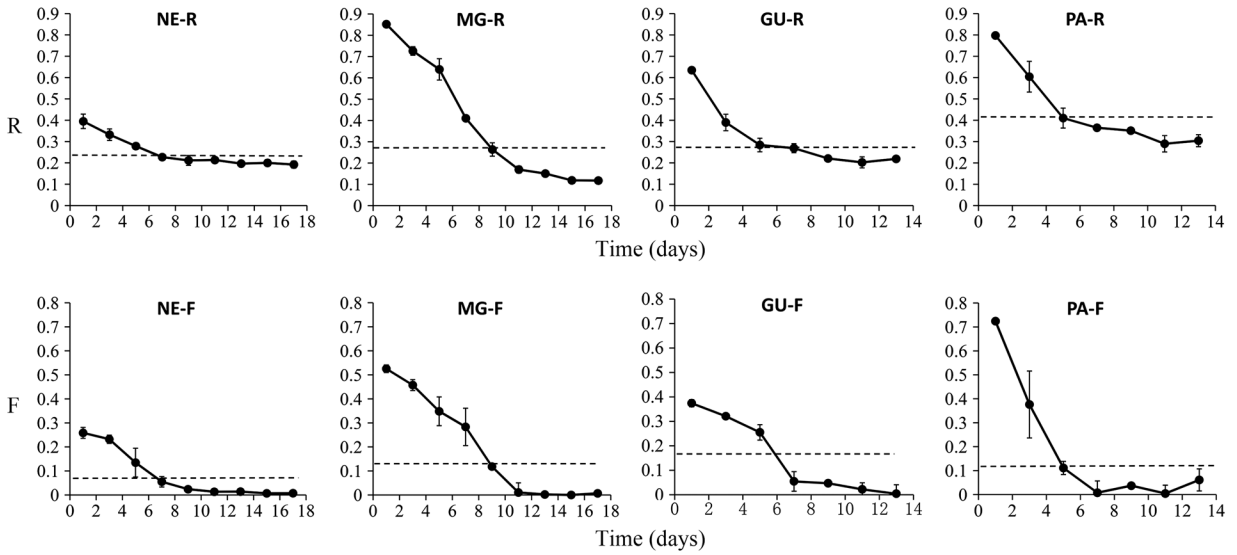

Fig. 6 The time evolution of the average *R* and *F* values for the fruits with standard deviation error bars indicated. Threshold values indicating the onset of full ripeness are given.

all kinds of fruits in this study does change (e.g., mango skin will change from green to yellow) when the fruits ripen gradually, which is induced by the breakdown of chlorophyll and the formation of additional pigments. With the visual appearance of the fruits and our experience, the fruits are ripe when *R* and *F* begin stabilizing, which means that the fruit quality will be acceptable to the consumer at this point. Here, we set a threshold value for each kind of fruit, which is indicated by the dashed lines in Fig. 6. It is clear that the change of skin color in fruit ripening must be reflected in a change in the values of *R* and *F*. The transition process combined with the threshold value is used to determine the time when the fruits are ripe. Due to some uncertainty and the statistical spread, there is clearly an uncertainty in the determination of the full ripeness day for different fruits. The time of ripeness can be inferred from the curves and the selected threshold values for all the fruits, as shown in Table 1. It should be noted that the absolute number of days does not have any significance here, since the prehistory of the fruits in the fruit dealers shop was unknown. The important aspect is that the ripeness of each kind of fruit can be assessed objectively with a quite small uncertainty using the function values and the set individual thresholds.

3.2 *Gas in Scattering Media Absorption Spectroscopy Measurements*

Since the injected laser power from the fiber was quite low in this study, a limited useful light propagation path resulted considering the reduction of light intensity due to absorption and scattering. Thus, rather than using transmission, the measurements were performed in a backscattering-like geometry with an injection-detection angular separation of 90°C, as can be seen in Fig. 1(b). Typical examples of acquired 2f signals of the four kinds of fruits are given in Fig. 7. It can be seen that the 2f signals for the fruits are quite good, so it is feasible to study changes of gas content inside the intact fruits during the fruit ripening.

Table 1 Day of onset of full ripeness for four kinds of fruits assessed with reflectance and fluorescence spectroscopies.

Type	Nectarine (NE)	Mango (MG)	Guava (GU)	Papaya (PA)
Day of onset of full ripeness	7 ± 1	9 ± 1	5 ± 1	5 ± 1

As a result of the strong scattering of light in fruits, the optical path length that the light travelled through the fruits is unknown, so straight-forward quantification of the oxygen concentration using the Beer–Lambert law is not applicable.[15] Instead, the equivalent mean path length, L_{eq}, is used to express the gas content. The L_{eq} value is the distance light would need to travel in normal air (21% oxygen) to result in the same fractional absorptive imprint on the received light intensity. L_{eq} is proportional to the normalized WMS signal (i.e., the 2f WMS signal amplitude divided by the light intensity received by the detector). Thus, L_{eq} is used to estimate the changes of oxygen content in fruits ripening in this study. Each sample was monitored five times consecutively every day, and the average derived L_{eq} was presented. The L_{eq} was measured as a function of time for the different fruits; see Fig. 8.

The time evolution of the oxygen equivalent mean path length shows a similar tendency for all fruits as seen in the figure. During the first days, the value of L_{eq} is found to decrease gradually to a minimum value, and then rise to a second peak. Eventually, it decreases to a very low value. In this process, the fruits are subjected to a series of physiological and biochemical changes. It should be noted that the changes in L_{eq} can be attributed to changes in oxygen concentration or in the path length through the gas, or both phenomena. A reason for the initial reduction of L_{eq} could be attributed to the changes of respiratory rate during fruit ripening. Because the four kinds of fruits are climacteric, the respiratory rate rapidly increases to a peak value (i.e., the climacteric point which is a stage of fruit ripening associated with maximum respiration rate and ethylene production) and then returns to or below the point before the event.[23,24] For the climacteric fruits, the climacteric point can be seen as the end point of the fruit ripening period. Then, the fruits are more susceptible to fungal invasion and begin to degrade, ultimately leading to cell death. It can be seen (Fig. 8) that the L_{eq} rises to a

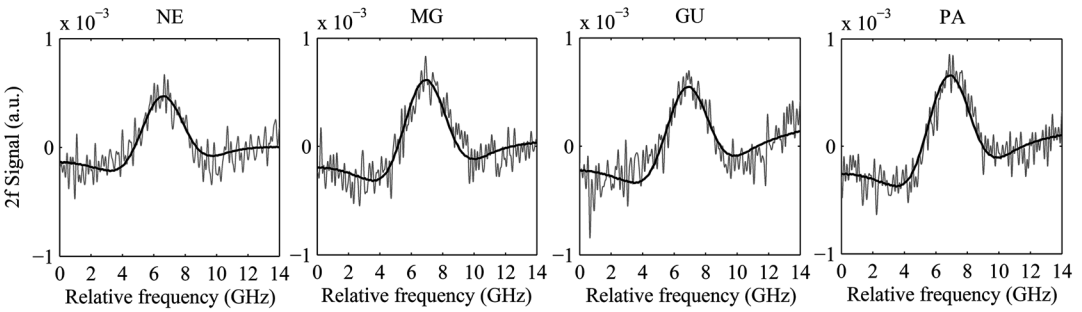

Fig. 7 Measured 2f signals (gray) and the fitted curve (black) for four kinds of fruits. The shapes used for fitting were attained by recording the high-quality 2f WMS oxygen signal for 1500 mm of free air.

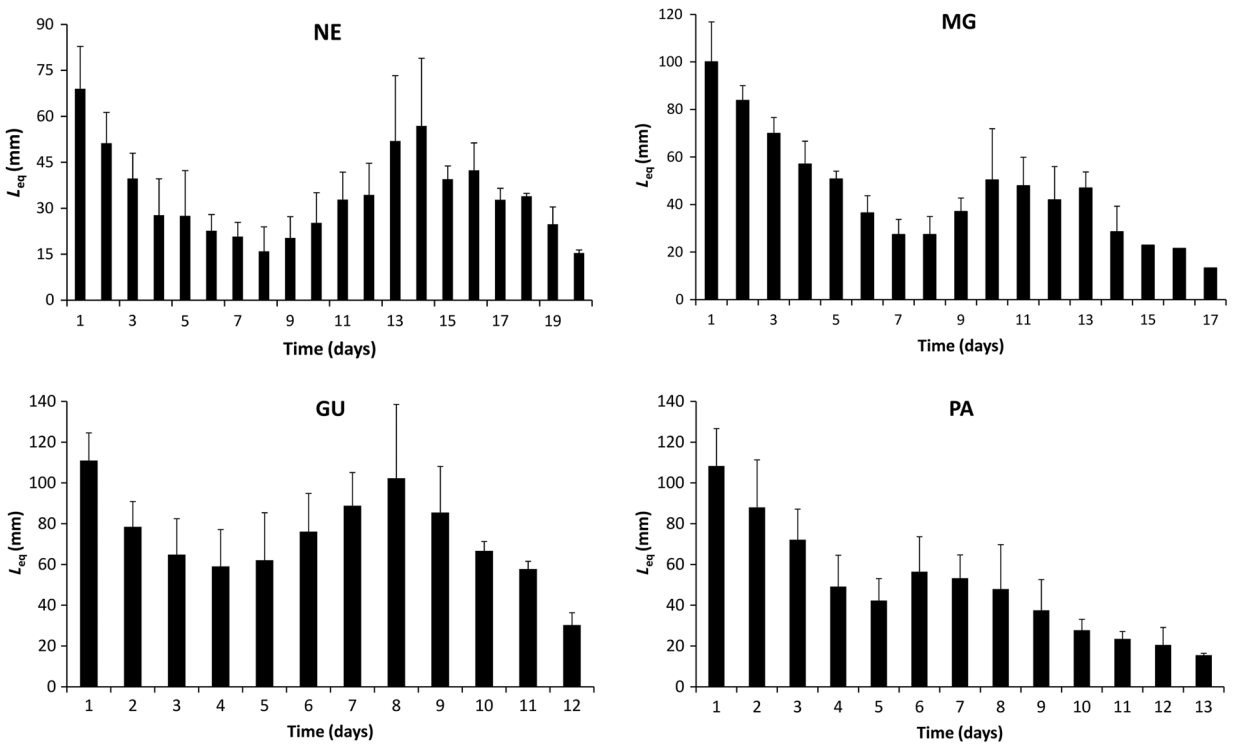

Fig. 8 The measured time evolution of the oxygen signal for nectarine, mango, guava, and papaya.

secondary peak and then decreases to a very low value after the climacteric point. This can be interpreted as due to the fact that the membrane structure is destroyed and the increasing membrane permeability makes the ambient air penetrate inside the aging fruits. Eventually, the fruits are decaying seriously and are filled with liquid replacing the air.[25] We note that the characteristic temporal variation of L_{eq} is useful for assessment of ripeness, regardless of detailed exploration. The day of full ripeness can be inferred from the time evolutions of the oxygen L_{eq} for the fruits, and can be associated with the occurrence of the initial minimum in the GASMAS signal. Also, considering the standard deviation errors, the results are shown in Table 2. We should note that from a practical point of view, on a particular measurement occasion it is not possible to locate the minimum of the curves shown in Fig. 8. However, again, since the GASMAS signal is monotonously falling in the interesting

Table 2 Day of onset of full ripening for four kinds of fruits as assessed from the minimum of the gas in scattering media absorption spectroscopy signal.

Type	Nectarine (NE)	Mango (MG)	Guava (GU)	Papaya (PA)
Day of onset of full ripeness	8 ± 1	8 ± 1	4 ± 1	5 ± 1

Table 3 The estimated number of days to the onset of full ripeness using a combination of the three spectroscopic techniques.

Type	Nectarine (NE)	Mango (MG)	Guava (GU)	Papaya (PA)
Number of days to onset of full ripeness	6 to 9	8 to 9	4 to 6	4 to 6

phase of the ripening process, we can again define individual threshold values for each kind of fruit, defining the initiation of full ripeness.

Combining Tables 1 and 2, the time duration during which the fruits can be considered to be progressing to full ripeness is estimated in Table 3 for each fruit type, using the combination of reflectance and fluorescence spectroscopies, as well as the GASMAS technique.

From Table 3, we note that the width in the period indicated becomes larger when combining the data. However, by setting thresholds more correctly based on experience of factual maturity these intervals could be narrowed down. What we have demonstrated is that the spectroscopic signals from all three methods are useful for estimating the degree of ripeness. Clearly, to get agreement with subjective maturity, the thresholds for individual kinds of fruits need to be firmly established. It seems that each of the spectroscopic techniques, or to gain more certainty, a combination thereof, could be quite useful to study fruit ripening and fruit quality. Useful shelf life might extend by a few days beyond the given time for the onset of full ripeness with basically non-impaired quality.

Ethylene, a gaseous organic compound in fruits and widely known to be involved in the ripening process, is not considered in our study. Especially for the climacteric fruits, large quantities of ethylene are produced during fruit ripening with a sharp increase of ethylene concentration occurring in connection with the reaching of the climacteric point for respiration.[24,26] The increasing ethylene level causes an increase in the respiration rate, accompanied by biochemical and physiological transformations during the ripening process. Therefore, the ethylene content together with oxygen can also be used as an indicator for fruit ripening.

4 Conclusions

The present results clearly show that it is possible to study the process of fruit ripening using nonintrusive optical methods. For fruit harvest and marketing, it is very important to know the maturity and full ripeness stages of the fruits. In this study, the changes of chlorophyll content were measured by reflectance and fluorescence spectroscopies, and the changes of oxygen concentration induced by respiration and other physiological processes were measured indirectly by the GASMAS technique. Analyzing the changes of these two parameters, the stage of fruit ripening could be obtained.

Acknowledgments

The authors are grateful to Liang Mei and Yuan Fu for assistance in setting up the GASMAS equipment. We are also grateful to Prof. Sailing He for kind support. This work was supported by the Guangdong Innovation Research Team Program (No. 201001D0104799318).

References

1. M. S. Reid, "Maturation and maturity indices," in *Postharvest Technology of Horticultural Crops*, A. A. Kader, Ed., 3rd ed., pp. 55–62, ANR Publication, University of California, USA (2002).
2. A. A. Kader, "Fruit maturity, ripening, and quality relationships," *Acta Hort. (ISHS)* **485**, 203–208 (1999).
3. C. H. Crisosto, "Stone fruit maturity indices: a descriptive review," *Postharvest News Inf.* **5**(6), 65–68 (1994).
4. G. Costa et al., "Internal fruit quality: how to influence it, how to define it," *Acta Hort. (ISHS)* **712**, 339–346 (2006).
5. V. A. McGlone, R. B. Jordan, and P. J. Martinsen, "Vis/NIR estimation at harvest of pre- and post-storage quality indices for 'Royal Gala' apple," *Postharvest Biol. Technol.* **25**(2), 135–144 (2002).
6. S. Saranwong, J. Sornsrivichai, and S. Kawano, "Prediction of ripe-stage eating quality of mango fruit from its harvest quality measured nondestructively by near infrared spectroscopy," *Postharvest Biol. Technol.* **31**(2), 137–145 (2004).
7. B. M. Nicolai et al., "Nondestructive measurements of fruit and vegetable quality by means of NIR spectroscopy: a review," *Postharvest Biol. Technol.* **46**(2), 99–118 (2007).
8. H. Cen and Y. He, "Theory and application of near infrared reflectance spectroscopy in determination of food quality," *Trends Food Sci. Technol.* **18**(2), 72–83 (2007).
9. E. Bonora, D. Stefanelli, and G. Costa, "Nectarine fruit ripening and quality assessed using the index of absorbance difference (IAD)," *Int. J. Agron.* **2013**, 242461 (2013).
10. V. Ziosia et al., "A new index based on VIS spectroscopy to characterize the progression of ripening in peach fruit," *Postharvest Biol. Technol.* **49**(3), 319–329 (2008).
11. F. Gottardi et al., "The index of absorbance difference (IAD) as a tool for segregating peaches and nectarines into homogeneous classes with different shelf-life and consumer acceptance," in *Proc. of the 8th Pangborn Sensory Science Symp.*, Firenze, Italy (2009).
12. S. Svanberg, *Atomic and Molecular Spectroscopy: Basic Aspects and Practical Applications*, 4th ed., Springer, Berlin (2004).
13. A. A. Gitelson and M. N. Merzlyak, "Signature analysis of leaf reflectance spectra: algorithm development for remote sensing of chlorophyll," *J. Plant Physiol.* **148**(3–4), 494–500 (1996).
14. K. Maxwell and G. N. Johnson, "Chlorophyll fluorescence—a practical guide," *J. Exp. Bot.* **51**(345), 659–668 (2000).
15. M. Sjöholm et al., "Analysis of gas dispersed in scattering media," *Opt. Lett.* **26**(1), 16–18 (2001).
16. L. Persson et al., "Studies of gas exchange in fruits using laser spectroscopic techniques," in *Proc. Frutic 05, Information and Technology for Sustainable Fruit and Vegetable Production*, pp. 543–552, Cemagref, Montpellier (2005).
17. L. Persson et al., "Diode laser absorption spectroscopy for studies of gas exchange in fruits," *Opt. Laser Eng.* **44**(7), 687–698 (2006).
18. M. Knee, *Fruit Quality and its Biological Basis*, Sheffield Academic Press, Sheffield (2002).
19. D. Wüstner et al., "Quantitative fluorescence loss in photobleaching for analysis of protein transport and aggregation," *BMC Bioinf.* **13**, 296–317 (2012).
20. T. Svensson et al., "VCSEL-based oxygen spectroscopy for structural analysis of pharmaceutical solids," *Appl. Phys. B* **90**(2), 345–354 (2008).
21. S. Svanberg, "Laser spectroscopy in medical diagnostics," in *Lasers for Medical Applications: Diagnostics, Therapy and Surgery*, H. Jelinkova, Ed., pp. 286–324, Woodhead Publishing, Cambridge (2013).
22. U. Rinderle and H. K. Lichtenthaler, "The chlorophyll fluorescence ratio F690/F735 as a possible indicator," in *Applications of Chlorophyll Fluorescence: In Photosynthesis Research, Stress Physiology, Hydrobiology and Remote Sensing*, H. K. Lichtenthaler, Ed., pp. 189–196, Springer, Berlin (1988).
23. H. A. Bashir and A.A. Abu-Goukh, "Compositional changes during guava fruit ripening," *Food Chem.* **80**(4), 557–563 (2003).
24. S. S. Zaharah et al., "Role of brassinosteroids, ethylene, abscisic acid, and indole-3-acetic acid in mango fruit ripening," *J. Plant Growth Regul.* **31**(3), 363–372 (2012).
25. S. P. Burg, *Postharvest Physiology and Hypobaric Storage of Fresh Produce*, 1st ed., CABI, London (2004).
26. P. Nath et al., "Role of ethylene in fruit ripening," in *Ethylene Action in Plants*, N. A. Khan, Ed., Springer-Verlag, Berlin (2006).

Hao Zhang received his bachelor's degree in physics from East China Institute of Technology, Nanchang, in 2011. His major field was optical engineering. He is now a PhD student at the Center for Optical and Electromagnetic Research at South China Normal University, Guangzhou. His current research interests concern applications of laser spectroscopy to the biophotonics field.

Jing Huang received her bachelor's degree at the Guangdong University of Technology in Guangzhou in 2012. She is now a master's student at the Center for Optical and Electromagnetic Research

at South China Normal University, Guangzhou. Her research interests include laser spectroscopy applied to food safety and biomedical topics.

Tianqi Li received her bachelor's degree in applied physics at Hefei University of Technology in 2013. She is now a master's student at the Center for Optical and Electromagnetic Research at the South China Normal University, Guangzhou. Her research interests include laser spectroscopy applied to food safety and biomedical topics.

Xiuxiang Wu received his bachelor's degree in optical information science and technology from the University of Jinan in 2011. His major field was optical engineering. He is now a master's student at the Center for Optical and Electromagnetic Research at South China Normal University, Guangzhou. His current research interests concern applications of laser spectroscopy to the environmental and biophotonics fields.

Sune Svanberg obtained his PhD from University of Gothenburg in 1972 and is since 1980 professor of physics at Lund University, Lund, Sweden. During 30 years, he was head of the Atomic Physics Division, and during 20 years director of the Lund Laser Centre. Since 2011, he is also a distinguished professor at the South China Normal University, Guangzhou. His research interests include laser spectroscopic applications to the environmental, food safety, and biomedical fields.

Katarina Svanberg obtained her PhD from Lund University in 1989 and is affiliated with the Department of Oncology, Lund University Hospital, where she has been active as chief consultant and professor of oncology for more than 25 years. Since 2011, she is also a distinguished professor at the South China Normal University, Guangzhou. She served as SPIE President in 2011. Her research interests concern applications of laser spectroscopy to the biomedical and biophotonics fields.